Remanent-magnetization reversal in nickel-manganese alloys

T. Satoh,* R. B. Goldfarb, and C. E. Patton

Department of Physics, Colorado State University, Fort Collins, Colorado 80523

Weakly ordered nickel-manganese alloys, field cooled to 4 K, exhibit a reversal in remanent magnetization upon warming. The reversal is dependent on the state of atomic order and the cooling field. A local-environment model and Mn-rich aggregates, which are isolated from other Mn-rich aggregates, explain the essential features of the reversal.

I. INTRODUCTION

Disordered Ni-Mn alloys near the stoichiometric Ni_3Mn composition exhibit a field-induced unidirectional anisotropy after field cooling to 4 K.[1] This results in a shifted hysteresis loop and a remanent magnetization which was explained by an exchange-anisotropy model[2,3] in which essentially macroscopic ferromagnetic regions are exchange coupled to antiferromagnetic regions.

In a recent study,[4,5] the present authors have obtained extensive data on the effect of composition, cooling field, measuring field, and degree of order on the magnetic properties of Ni-Mn alloys from 22- to 32-at.% Mn. For the disordered alloys, the susceptibility results showed an antiferromagnetic character for Mn content above 25 at.% and a ferromagnetic character for Mn content below 25 at.%. From observations of the measuring field at 4 K required to overcome the exchange anisotropy in zero-field-cooled alloys, the exchange-anisotropy field was found to increase from 10 kOe at 22-at.% Mn to 90 kOe at 32-at.% Mn, for the disordered alloy. Weak partial ordering decreased the anisotropy field. These results were explained by a local-environment model (LEM), proposed by Satoh *et al.*,[4] which considers the nearest-neighbor environment (NNE) of Mn attoms in the alloy.

As recently reported,[6] a remanence reversal effect has been found in these alloys. The remanent magnetization M_r, which results after cooling in a field to 4 K, decreases upon warming and changes sign between 40 and 200 K; i.e., the direction of M_r becomes opposite to the direction of the initial cooling field. The effect appears to be largest for the 25-at.%-Mn composition and weak atomic ordering. This remarkable effect was also explained in terms of the LEM. In the present study, the remanence reversal effect was investigated as a function of cooling field, order development due to annealing at 500 °C, and composition. The data are discussed in relation to calculations based on the LEM.

II. EXPERIMENT

The alloy samples were cast into ingots in an argon atmosphere after rf induction melting. The ingots were homogenized by cold working and quenching from 1000 °C several times. Spherical samples for measurement, 2.5–3.0 mm in diameter, were fabricated by a modified two-pipe lapidary method. Compositions were determined by atomic absorption methods on pieces in close proximity to the region in the ingot from which the spherical samples were cut. The samples were atomically disordered by vacuum sealing them in thin-walled quartz tubes (3-mm i.d. and 0.5-mm wall thickness), holding them at 1000 °C for 3 h, and quenching in ice water. Thermocouple measurements indicated that the time spent in the ordering temperature range from 600 to 350 °C, during the quenching process, was about 3 sec. Neutron diffraction did not detect the presence of any appreciable atomic order for rod samples quenched in this manner.[7]

Magnetization was measured by standard vibrating sample magnetometry. The samples were initially cooled to 4 K in the presence of an external cooling field. Two separate systems were used for the low-field and high-field cooling experiments. For cooling fields from zero to 8 kOe, a conventional iron yoke electromagnet and a Princeton Applied Research Model FM1 magnetometer were used with a Janis Varitemp dewar. Prior to measuring the relatively weak remanence, the electromagnet was removed from the vicinity of the sample. The remanent magnetization was measured as the temperature was raised continuously from 4 K to room temperature. Current to the temperature controller heating element was switched off during the actual measurement to avoid noise. Two measurements were made at each temperature, one with the sample rotated 180° to cancel any effect of asymmetry in the pick-up coils, the sample position, or stray fields. For cooling in high field (56 kOe), a superconducting solenoid with a Princeton

Applied Reserach Model 150A parallel field magnetometer and a Janis Varitemp dewar were used. For this system, the magnet was switched off after field cooling and before the remanence was measured as a function of increasing temperature. The reversal in remanence was distinct at both facilities.

The compositions analyzed were 22.1, 24.6, 26.2, 29.0, and 32.1-at.% Mn. The samples used were in the disordered state, in states of partial order, or ordered for 50 h at 500 °C. States of partial order were obtained by annealing a disordered sample at 500 °C for various periods of time while vacuum sealed in thin-wall quartz, followed by an ice water quench. The annealing was taken to be cumulative.

III. EXPERIMENTAL RESULTS

As established by the early work of Kouvel and co-workers,[1] disordered Ni-Mn alloys near the Ni_3Mn composition exhibit a remanent magnetization in the field direction after field cooling to 4 K. Figure 1 shows a typical hysteresis loop for the disordered 24.6-at.%-Mn alloy at 4 K after cooling in 8 kOe. The magnetization curve shows very little hysteresis and is shifted to yield a single unidirectional remanence $M_r^{initial}$ in the direction of the cooling field H_{cool}. It is this induced remanence which is examined as a function of temperature during warming in this study. This shifted magnetization curve is a well-known characteristic of unidirectional anisotropy. The magnetization curve for cooling in zero field, denoted by $H_{cool} = 0$, is also shown. This curve shows no shift, no remanence, and a much smaller magnetization for a given measuring field.
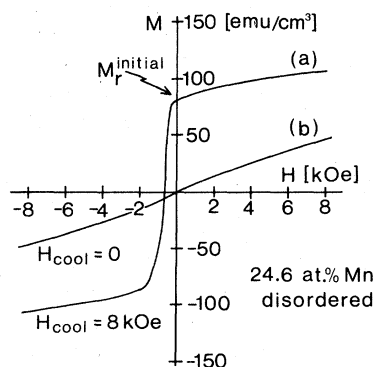
The first observation of remanence reversal was

FIG. 1. Magnetization M vs applied field H at 4 K for a disordered 24.6-at.%-Mn alloy after field cooling in 8 kOe [$H_{cool} = 8kOe$, curve (a)] and in zero field [$H_{cool} = 0$, curve (b)]. The positive M axis is in the initial cooling field direction.
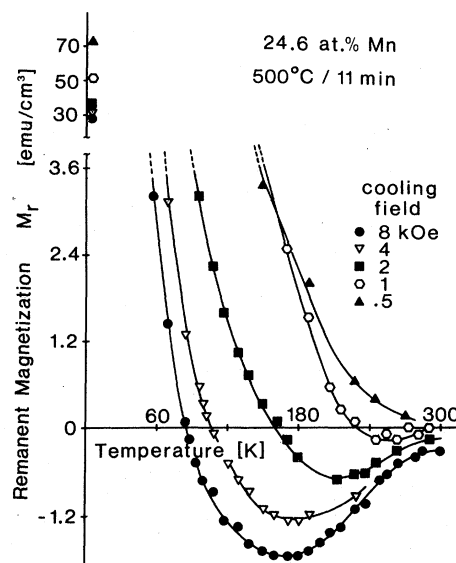

FIG. 2. Remanent magnetization M_r as a function of temperature during warming from 4 K after cooling from 300 to 4 K in various fields as indicated. The data are for a 24.6-at.%-Mn sample, initially disordered by rapid quenching from 1000 °C, and then partially ordered by holding at 500 °C for 11 min.

for this 24.6-at.%-Mn composition with a small amount of order development induced by briefly annealing the sample at 500 °C. In Fig. 2 the effect is shown for a fixed annealing time of 11 min and for various cooling fields. The remanence at 4 K induced by the field cooling decreases upon warming, crosses zero, and becomes negative at higher temperatures. The direction of the reversed moment is found to be exactly antiparallel, at an angle of 180°, relative to the initial cooling field direction. The crossover temperature T_0, where M_r is zero, decreases with increasing H_{cool}. The maximum reversed remanence, $M_r^{rev-max}$, increases with increasing cooling field. It is of interest to note that the initial remanence at 4 K decreases with increasing cooling field, opposite to the exchange anisotropy prediction. These results are not explained by the currently accepted exchange anisotropy model.

Figure 3 summarizes the dependences upon cooling field of the initial remanence at 4 K, $M_r^{initial}$, the crossover temperature for zero remanence T_0, and the maximum reversed remanence $M_r^{rev-max}$. The data for $M_r^{initial}$ show that the remanence at 4 K is a decreasing function of cooling field. For $H_{cool} = 0$, however, the initial remanence is zero. This result indicates that the cooling field dependence of $M_r^{initial}$ is quite different from that for the disordered alloy, for which $M_r^{initial}$ increases smoothly from zero with increasing H_{cool}. The crossover temperature T_0 decreases with increas-
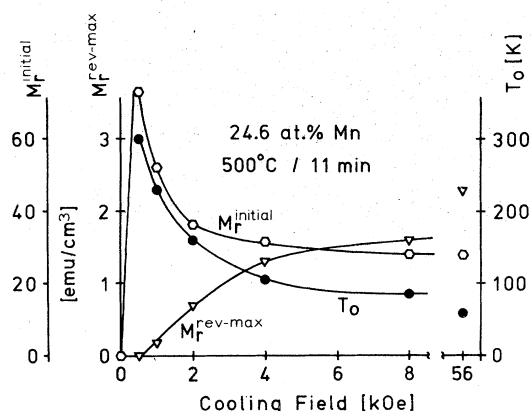
FIG. 3. Initial remanence at 4 K, M_r^{initial}, the maximum reversed remanence $M_r^{\text{rev-max}}$ during warming, and the crossover temperature for zero remanence T_0 as a function of the cooling field, for the data in Fig. 2.

ing cooling field, while $M_r^{\text{rev-max}}$ increases smoothly with cooling field. These results and their implications will be considered in Sec. IV.

Figure 4 shows the temperature dependence of the remanence after field cooling in a fixed field of 8 kOe, with the annealing time at 500 °C as a parameter, for the 24.6 at.%-Mn alloy. The reversal
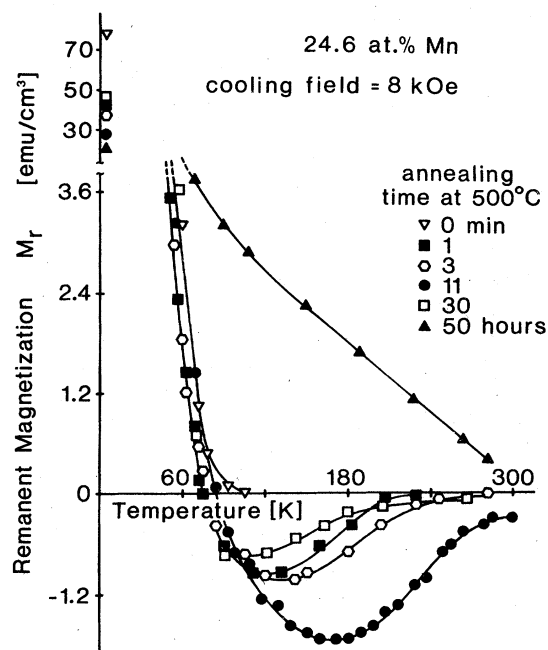

FIG. 4. Remanent magnetization M_r as a function of temperature during warming from 4 K after cooling from 300 to 4 K in 8 kOe. The data are for 24.6-at.%-Mn alloy samples, initially disordered by rapid quenching from 1000 °C, and then partially ordered by holding at 500 °C for the cumulated times indicated.
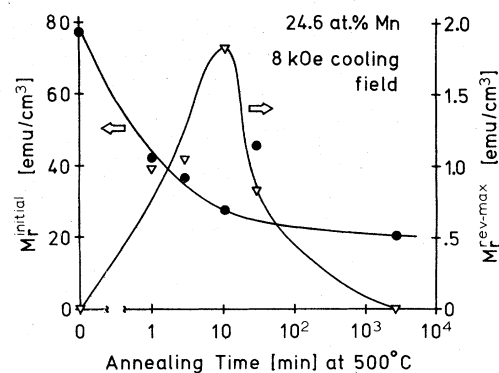

FIG. 5. Initial remanence at 4 K after cooling from 300 K in 8 kOe, M_r^{initial}, and the maximum reversed remanence upon warming $M_r^{\text{rev-max}}$, as a function of annealing time at 500 °C for an initially disordered 24.6-at.%-Mn alloy, based on the data in Fig. 4.

effect is clearly in evidence for all but the disordered and 50-h ordered samples. It is noteworthy that the crossover temperature is insensitive to the degree of order (in partially ordered alloys) and that the maximum reversed remanence shows a maximum for a partially ordered state. These two characteristics are key points to be considered closely in Secs. IV and V. Figure 5 summarizes the dependences upon annealing time of the initial remanence M_r^{initial} and the maximum reversed remanence $M_r^{\text{rev-max}}$. The initial remanence simply decreases with annealing time, while the maximum reversed remanence goes through a peak at about 11 min in the case of 500 °C annealing.

As evident from Figs. 2 and 4, the remanence reversal effect is quite small. The reversed remanence is more than an order of magnitude smaller than the initial remanence at 4 K after field cooling. Apart from the 24.6-at.%-Mn sample, remanence reversal was also observed in a disordered 22.1-at.%-Mn sample under high-field-cooling conditions. Figure 6 shows the data for field cooling in 56 kOe. The reversal effect is distinct but extremely small. The crossover is near 40 K. This is the smallest T_0 observed in these experiments. Data for the 24.6-at.%-Mn sample, annealed 11 min at 500 °C, are also shown. The initial decrease in M_r is sharper than for cooling in lower fields. No reversal was found for the alloys with Mn content above 25 at.%.

The results presented above are summarized in Table I. The three magnetic parameters that serve to describe remanence reversal are listed, along with the effect of cooling field and partial ordering on them. The initial remanence M_r^{initial}, obtained after cooling in a field to 4 K, is found to decrease with increasing cooling field (in partially ordered alloys) and decrease with order develop-
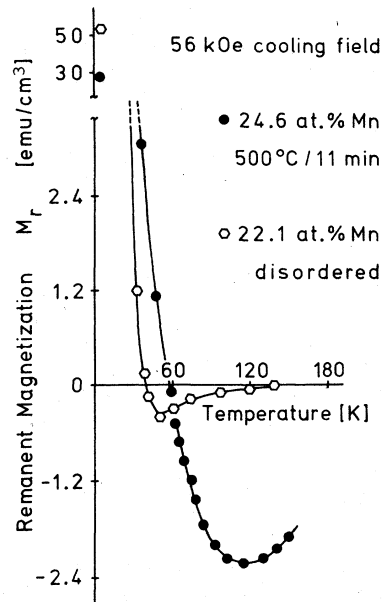
FIG. 6. Remanent magnetization M_r as a function of temperature during warming from 4 K after cooling from 300 to 4 K in 56 kOe for two samples: a 24.6-at.%-Mn alloy annealed for 11 min at 500 °C from a disordered state, and a 22.1-at.%-Mn alloy in the disordered state.

ment. The crossover temperature T_0, for zero remanence upon warming from 4 K, is found to decrease with increasing cooling field and to be virtually independent of the state of atomic order for partially ordered samples. The maximum reversed remanence, $M_r^{\text{rev-max}}$, increases with cooling field and peaks for an annealing time of 11 min at 500 °C, which corresponds to a state of partial order development.

IV. LOCAL-ENVIRONMENT MODEL AND REMANENCE REVERSAL

The results outlined in Sec. III can be qualitatively explained by the LEM.[4-6] Moreover, the dependence of the maximum reversed remanence $M_r^{\text{rev-max}}$ on annealing time and the peak at an intermediate state of order can be quantitatively ex-

plained by a statistical calculation based on this model. In this section remanence reversal is interpreted in terms of the LEM. In Sec. V the theoretical calculation is described.

In the LEM, Mn atoms are classified according to their NNE. One type Mn(A) has a Mn-rich NNE and is coupled antiferromagnetically to its Mn nearest neighbors. These Mn(A) aggregates have a relatively high Néel temperature. The second type Mn(B) has a NNE corresponding to a local composition of 25-at.% Mn. The Mn(B) is exposed to a very weak molecular field. The third type Mn(C) has a Mn deficient NNE and is ferromagnetically coupled to its Mn and Ni nearest neighbors.[8] The Mn(A) atoms appear to be important in remanence reversal and will be the focus of the LEM discussion here.

Mn(A) atoms are those Mn atoms which have four or more nearest-neighbor Mn atoms in their NNE. Figure 7(a) shows a core Mn(A) atom with four such neighbors; the remaining atoms in the NNE are nickel atoms. It is assumed that when the Mn NNE contains four or more Mn atoms as for Mn(A), the NNE magnetic moments are (i) coupled parallel within themselves, and (ii) coupled antiparallel to the core Mn(A) atom. This assumption is plausible, since nearest-neighbor Mn atoms have an antiferromagnetic exchange interaction and sufficient Mn atoms in the NNE should allow this tendency to dominate over the ferromagnetic Ni-Mn nearest neighbor exchange. The presence of Mn spins coupled antiparallel to their environmental spins has been directly observed using NMR techniques by Kitaoka and Asayama.[9] Thus, the Mn(A) regions may be viewed as a ferromagnetic Mn-rich NNE shell which is coupled antiferromagnetically to the Mn(A) core atom.

Consider the magnetic history which leads to remanence reversal in light of this model. During field cooling, the ferromagnetic NNE with a relatively large net moment is aligned with the cooling field. There is a Néel temperature T_N related to the net antiferromagnetic interaction between the Mn(A) and its NNE. As the temperature during field cooling falls below the T_N for a particular

TABLE I. Summary of experimental results on remanence reversal. Crossover and reversal occur in Ni-Mn alloys which are partially ordered.

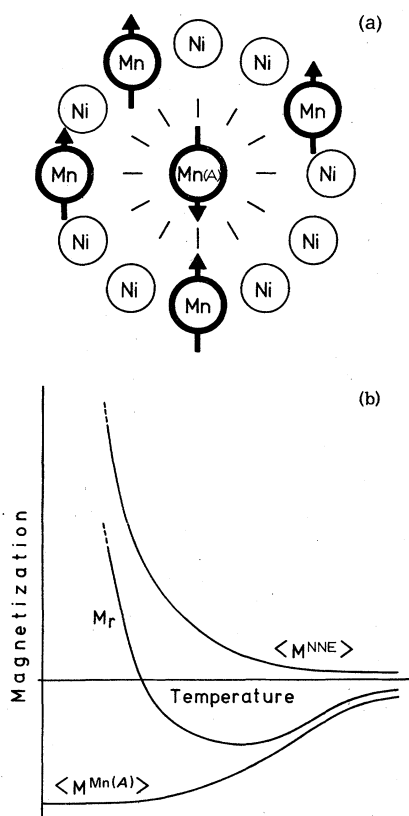| Parameter	Cooling-field dependence	Atomic-order dependence
Initial 4 K remanence M_r^{initial}	Decreases in partially ordered alloys	Decreases
Crossover temperature T_0	Decreases	Independent
Maximum reversed remanence $M_r^{\text{rev-max}}$	Increases	Peaks for a partial-order state

FIG. 7. (a) Schematic representation of a Mn (A) local aggregate within the context of the LEM. The core Mn atom has four nearest-neighbor Mn atoms in its NNE. The NNE moments are all parallel, and antiparallel to the Mn(A) moment. (b) Schematic representation of the magnetization contributions of the NNE, $\langle M^{NNE} \rangle$, and the Mn(A), $\langle M^{Mn(A)} \rangle$ to the remanent magnetization as a function of temperature. Reversal occurs for temperatures where $\langle M^{NNE} \rangle < \langle M^{Mn(A)} \rangle$ is satisfied.

Mn(A) region, that Mn(A) core moment will be aligned opposite to the field and the local spin order will freeze-in. The NNE moments will be frozen-in along the cooling field direction; the Mn(A) moment will be frozen-in opposite to this direction. The initial remanence $M_r^{initial}$ at 4 K is due to the field aligned and relatively large NNE moment.

Now, examine the behavior of the field induced remanence during warming. If the average NNE moment falls off more rapidly than does the average Mn(A) moment, one may obtain a compensation point in the remanence. Remanence reversal will occur if, in addition, the net coupling between the core Mn(A) atom and the NNE remains antiferromagnetic along the initial axis of the field cooling. Such behavior is realized if the coupling of the Mn(A) core atoms to their NNE is stronger than that of the NNE atoms to *their* environment. A

qualitative variation of these moments with temperature which would lead to crossover and remanence reversal is shown in Fig. 7(b). The small high-temperature tail for the NNE magnetization is included to indicate the small residual coupling which is necessary for the Mn(A) magnetization to "remember" the initial field cooling history and to overcome thermal agitation. For remanence reversal to occur, it is necessary (i) for the NNE magnetization to become very small, relative to its 4-K value, above crossover, while (ii) still preserving the antiferromagnetic coupling to the Mn(A). Subject to these conditions, it is possible to obtain a true remanence reversal opposite to the cooling field direction for any cooling field orientation. The direction of the Mn(A) moments is not influenced by the crystalline anisotropy within the individual crystallites. From the recent data by Iwata *et al.*[10] for single crystal Cu-Mn, the exchange anisotropy and initial field cooled remanence are independent of the crystallographic orientation and depend only on the magnitude and direction of the cooling field.

The LEM explains the essential features of the data presented in Sec. III. First, consider the behavior of the initial remanence. Within the framework of the LEM, the cooling field should have two effects: (i) The field will serve to better align the ferromagnetic NNE and thereby increase $M_r^{initial}$. (ii) As the NNE is better aligned, however, the antiferromagnetic coupling between the Mn(A) and the NNE causes the Mn(A) to be better aligned, and this will tend to reduce the initial field cooled remanence at 4 K. The curve in Fig. 3 shows that for 24.6-at.% Mn annealed at 500 °C for 11 min, $M_r^{initial}$ increases rapidly from zero at $H_{cool} = 0$ to 73 emu/cm^3 at $H_{cool} = 0.5$ kOe, and decreases for larger cooling fields. A reasonable explanation is that the initial rapid increase is due to the alignment of the relatively soft ferromagnetic NNE. The more gradual falloff for larger cooling fields is due to the enhanced Mn(A) alignment, which serves to reduce the initial remanence.

The enhanced alignment of the Mn(A) opposite to the NNE magnetization and cooling field direction also explains the effect of cooling field on the crossover temperature and the maximum reversed remanence. If, as proposed above, larger cooling fields promote a better antiparallel alignment of the Mn(A) core spins, the compensation between the NNE and Mn(A) moments will occur at a lower temperature. T_0 is, in fact, observed to decrease with increased cooling field as discussed in conjunction with Figs. 2 and 3. This enhanced Mn(A) magnetization also causes the maximum reversed remanence to increase as the cooling field is increased. This expectation agrees with the data in
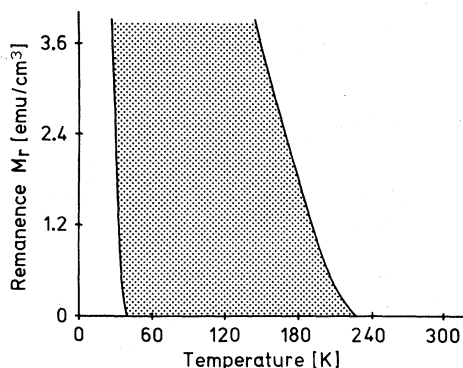
FIG. 8. Critical region for remanence vs temperature, upon warming from 4 K after field cooling, for which remanence reversal can occur.

Fig. 3.

Within the framework of the LEM, which is a kind of Ising model, one would consider that the opposing moments must have appropriate magnitudes and temperature dependence if remanence reversal is to occur. From a consideration of the data in Figs. 2, 4, and 6, one arrives at the observation that the initial decrease in the positive remanence upon warming should fall in the shaded area of Fig. 8, if remanence reversal is to occur. If the NNE moment decreases more rapidly, the Mn(A) spin is no longer supported by the NNE and no reversal is possible. Disordered and nickel-rich alloys have such curves. The 22.1-at.%-Mn data in Fig. 6 indicate that 40 K is a reasonable low-temperature limit for reversal to occur. If, on the other hand, the NNE moment decreases very slowly upon warming it would never fall below the Mn(A) moment and no reversed remanence could occur. Samples with a large amount of atomic order, samples with high Mn content, and samples cooled in very small fields have such curves.

V. THEORY FOR MAXIMUM REVERSED REMANENCE

The effect of annealing time on crossover and $M_r^{\text{rev-max}}$ provides the most important connections between the LEM and the present data. It is presumed, based on the magnetization versus temperature data in Ref. 4, that there is actually a distribution of T_N values for Mn(A) cores with different NNE configurations. Figure 4 shows, however, that the crossover is quite insensitive to annealing time. This result suggests that the individual Mn(A) atomic regions which are responsible for the remanence reversal, are not modified by the ordering process. The concentration of these regions, however, is a sensitive function of annealing time. This is reflected in the data of Figs.

4 and 5, which show that the maximum reversed remanence first increases with ordering, up to an annealing time of 11 min at 500 °C, and then decreases for longer annealing times.

As mentioned above, the Mn(A) atomic aggregates provide a reasonable explanation of remanence reversal. However, the concentration of Mn(A) aggregates obviously decreases with increasing atomic order while the remanence reversal peaks for an intermediate order state as shown in Figs. 4 and 5. The constant crossover temperature in Fig. 4, which is independent of the amount of atomic order, suggests that only one particular class of Mn(A) aggregates is responsible for remanence reversal. Such aggregates must have a statistical concentration appropriate to the observed magnitude of $M_r^{\text{rev-max}}$ and that concentration must also go through a maximum at an appropriate intermediate order state.

A particular class of Mn(A) regions, termed isolated Mn(A), has been found to have these properties and to quantitatively account for remanence reversal. In the analysis, then, it is necessary to distinguish between different types of Mn(A) aggregates. The distinction is in terms of the NNE of the Mn atoms in the NNE of the core Mn(A) atom. Recall that Mn(A) atoms are those for which four or more of the twelve nearest-neighbor atoms are manganese. At the extreme, isolated Mn(A) atoms are those for which none of the nearest-neighbor Mn atoms are themselves in the Mn(A) category. For these isolated Mn(A) aggregates, it is expected that the qualitative arguments of Sec. IV are valid, with a ferromagnetic NNE shell coupled antiferromagnetically to the core Mn(A) atom. These regions are proposed to be responsible for remanence reversal. The purpose of this section is to describe a quantitative calculation of the variation in the concentration of the various types of Mn(A) aggregates with atomic order. The results are then related to the present data on remanence reversal. Finally, the possible role of *multiple* Mn(A) aggregates, those with Mn(A) atoms in their NNE, is briefly considered.

An atomic site in the fcc lattice which contains a manganese atom, and n nearest-neighbor manganese atoms, out of the possible twelve nearest-neighbor atoms, as illustrated in Fig. 7(a) for $n = 4$, will occur with a probability

$$P_{\text{Mn}}^{(n)} = x[12! / n! (12 - n)!](1 - p)^n p^{12-n} . \qquad (1)$$

In Eq. (1) p is the probability that a given Mn nearest-neighbor atom will be a Ni atom, and x is the fraction of Mn atoms per formula unit $\text{Ni}_{1-x} \text{Mn}_x$.

The probability p is related to the sample composition and degree of atomic order. Since only

the nearest neighbor environment is examined, it is appropriate to employ a short-range-order parameter σ in the analysis,

$$\sigma = (p - p_{\text{disord}})/(p_{\text{ord}} - p_{\text{disord}}) . \tag{2}$$

The subscripts "disord" and "ord" refer to the probability that a given manganese nearest neighbor is nickel for disordered and perfectly ordered states, respectively. These probabilities are given by

$$p_{\text{ord}} = 1, \quad x \leqslant 0.25 , \tag{3a}$$

$$p_{\text{ord}} = 1.25 - x, \quad x \geqslant 0.25 , \tag{3b}$$

$$p_{\text{disord}} = 1 - x . \tag{4}$$

From the above relations, the existence probability of a Mn atom with different NNE can be calculated as a function of composition x and short-range-order parameter σ.

For the Mn(A) category, which is central to the application of the LEM to remanence reversal, one may calculate,

$$P_{\text{Mn}}^{(A)}(x, \sigma) = \sum_{n=4}^{12} P_{\text{Mn}}^{(n)}(x, \sigma) , \tag{5}$$

the existence probability for Mn atoms with four or more nearest-neighbor Mn atoms. These regions are of importance in exchange anisotropy and related phenomena.[4,5] Here arises the problem that Mn atoms in the NNE can also be nearest neighbors to other Mn atoms in the NNE. Since the Mn concentration is not dilute, such complications are of importance. They are, however, neglected in the present analysis for convenience of calculation.

As discussed above, it is necessary to consider isolated Mn(A) regions explicitly. Expressions for the existence probability of these regions can be obtained by considering explicitly the Mn atoms in the NNE of the core Mn(A) in Fig. 7(a). There are four to twelve such atoms; each one already has at least one nearest-neighbor Mn atom in the core Mn(A) atom. For this reason, the counting procedure is modified from that utilized above. Out of the eleven remaining nearest neighbors of the Mn in the NNE, the probability that m of them are also Mn is

$$Q_{\text{Mn}}^{(m)}(x, \sigma) = [11!/m!(11 - m)!](1 - p)^m p^{11-m} . \tag{6}$$

The existence probability of a Mn(A) core with a certain number of Mn atoms in its NNE, specified by n, and with z of these n Mn atoms also Mn(A), is given by

$$R_{\text{Mn}}^{(n, z)} = P_{\text{Mn}}^{(n)}(x, \sigma) \frac{n!}{z!(n - z)!} \left(\sum_{m=3}^{11} Q_{\text{Mn}}^{(m)} \right)^z$$

$$\times \left(\sum_{m=0}^{2} Q_{\text{Mn}}^{(m)} \right)^{n-z} . \tag{7}$$

Thus, the existence probability of isolated Mn(A) aggregates is obtained as

$$P_{\text{Mn}(A)}^{\text{isol}} = \sum_{n=4}^{12} R_{\text{Mn}}^{(n, z=0)} . \tag{8}$$

The existence probability of multiple Mn(A) aggregates, those with one or more Mn(A) atoms in the NNE, is given by

$$P_{\text{Mn}(A)}^{\text{mult}} = \sum_{n=4}^{12} \sum_{z=1}^{n} R_{\text{Mn}}^{(n, z)} . \tag{9}$$

The calculated existence probability for isolated Mn(A) aggregates and multiple Mn(A) aggregates are shown as a function of the short-range-order parameter σ in Fig. 9, for $x = 0.25$. The isolated Mn(A) regions initially increase in concentration up to $\sigma \approx 0.4$ and then decrease for $\sigma > 0.4$. The multiple Mn(A) regions simply decrease with increasing σ as order development breaks up nearest-neighbor Mn pairs. As the multiple Mn(A) regions break up during the initial stages of ordering, an increase in the number of isolated aggregates results. For example, one may imagine a process where twin Mn(A) aggregates with $z = 1$ decay into isolated Mn(A) regions. Wide-scale order development will eventually lead to a decrease in all types of Mn(A) aggregates.

Comparison of the theoretical results in Fig. 9 with the data in Fig. 5 provides support for the interpretation of remanence reversal in terms of the LEM. Consider first the size of the maximum reversed remanence at the peak, 2.2 emu/cm^3, for the 24.6-at.%-Mn alloy annealed for 11 min at 500 °C (Fig. 6). If the peak is due to the isolated Mn(A) regions, the maximum reversed remanence is given by

$$M_r^{\text{rev-max}} = 4 \mu_{\text{Mn}} P_{\text{Mn}(A)}^{\text{isol}} / a_0^3 , \tag{10}$$

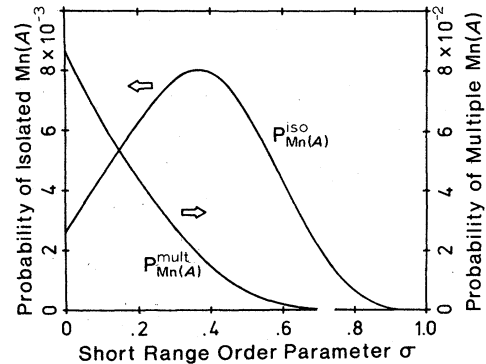where μ_{Mn} is the moment per Mn(A) atom, a_0 is

FIG. 9. Calculated existence probability for isolated Mn(A) regions, $P_{\text{Mn}(A)}^{\text{isol}}$, and multiple Mn($A$) regions, $P_{\text{Mn}(A)}^{\text{mult}}$, as a function of short-range-order parameter σ for the Ni$_3$Mn composition.

the lattice constant and the factor of 4 accounts for the four atoms per unit cell in the fcc lattice. For $a_0 = 3.59$ Å and $M_r^{\text{rev-max}} \approx 2.2$ emu/cm^3, one obtains a value of the Mn(A) moment,

$$\mu_{\text{Mn}} \approx 0.34 \mu_B . \tag{11}$$

Kitaoka and Asayama[9] estimate a value of 1.6–1.7 μ_B for the antiparallel Mn atoms in an alloy of 10-at.% Mn. They suggest that manganese NNE atoms can cause a reduction in the core Mn moment. The neutron data of Cable and Child[11] for disordered Ni-Mn alloys with Mn content up to 20 at.% also indicate a strong decrease in the average Mn moment with increasing Mn content. They suggest an environmental effect on the Mn atomic moment. Recall that the reversed remanence is due to the difference between the Mn(A) moment and the NNE moment. Equation (10) assumes that the NNE moment is negligible at the temperature where the reversed remanence is maximum. Thus, the 0.34 μ_B estimate for the moment of the isolated Mn(A) core is reasonable.

The dependence of the remanence reversal upon annealing time in Fig. 5 is also consistent with the theoretical results for isolated Mn(A) in Fig. 9. If one assumes a simple thermal diffusion process for the atomic order development, the horizontal axis in Fig. 5 is linear in the order parameter σ. For thermal equilibrium at 10^4–10^5 min, the peak in the reversed remanence is estimated to occur at $\sigma \approx 0.3$–0.4. The peak in the concentration of isolated Mn(A) aggregates in Fig. 9 is seen to occur at $\sigma \approx 0.4$. Thus, the isolated Mn(A) aggregate concept, ·although the correlation with the NNE is neglected, explains both the maximum reversed remanence and its dependence upon atomic order. A complete LEM analysis would require identification of the explicit nature of the Mn(A) regions responsible for remanence reversal, as well as a more rigorous statistical calculation.

The role of various types of multiple Mn(A) re-

gions should also be considered. Twin Mn(A) regions, in which the Mn(A) core has one Mn(A) atom in its NNE, might freeze-in with the two core Mn(A) moments parallel due to the effect of the rest of the NNE, in spite of the negative exchange between them. Upon warming under zero-field conditions, these spins could return to their antiparallel orientation and diminish the magnitude of the remanence reversal. For triplets and higher-order multiple Mn(A) aggregates, one would expect the antiferromagnetic interactions to dominate the spin order within the aggregate. The net moment of such multiple Mn(A) regions would be zero, and they would not contribute to the remanence reversal.

VI. SUMMARY AND CONCLUSION

A comprehensive experimental characterization of remanence reversal in Ni-Mn alloys has been made. The data have been explained on the basis of a LEM. The reversal is due to isolated Mn(A) atoms with four or more Mn nearest neighbors, none of which are themselves Mn(A) atoms. The model accounts for the reversed remanence and its dependence on atomic order. It also explains other essential features. The remanence reversal may be considered as a second-order effect related to the LEM, just as the exchange anisotropy and related phenomena considered in Refs. 4 and 5 are first-order effects of the LEM.

*Present address: The Electrotechnical Laboratory, Tanashi, Tokyo, Japan.
[1]J. S. Kouvel and C. D. Graham, Jr., J. Phys. Chem. Solids 11, 220 (1959).
[2]W. H. Meiklejohn and C. P. Bean, Phys. Rev. 105, 904 (1957).
[3]J. S. Kouvel, J. Phys. Chem. Solids 24, 795 (1963).
[4]T. Satoh, C. E. Patton, and R. B. Goldfarb, AIP Conf. Proc., 34, 361 (1976).
[5]T. Satoh, R. B. Goldfarb, and C. E. Patton, J. Appl. Phys. 49, 3439 (1978).
[6]T. Satoh, R. B. Goldfarb, and C. E. Patton, Proceedings of the International Conference on Magnetism, Amsterdam, 1976 (unpublished); Physica B (Netherlands) 86-88B, 820 (1977).

[7]J. J. Rhyne (private communication).
[8]T. Jo, J. Phys. Soc. Jpn. 40, 715 (1976), has also hypothesized the existence of antiferromagnetically coupled Mn atoms based on the results of a coherent-potential-approximation calculation. Antiparallel Mn spins are also discussed by J. W. Cable and H. R. Child, J. Phys. Suppl. (Paris) C 1, 67 (1971), and by M. J. Marcinkowski and R. M. Poliak, Philos. Mag. 8, 1023 (1963).
[9]Y. Kitaoka and K. Asayama, J. Phys. Soc. Jpn. 40, 1521 (1976).
[10]T. Iwata, K. Kai, T. Nakamichi, and M. Yamamoto, J. Phys. Soc. Jpn. 28, 582 (1970).
[11]J. W. Cable and H. R. Child, Phys. Rev. B 10, 4607 (1974).